Photoluminescence enhancement of ZnO via coupling with surface plasmons on Al thin films

S. Dellis, N. Kalfagiannis, S. Kassavetis, C. Bazioti, G. P. Dimitrakopulos, D. C. Koutsogeorgis, and P. Patsalas

Citation: Journal of Applied Physics **121**, 103104 (2017); doi: 10.1063/1.4977954
View online: http://dx.doi.org/10.1063/1.4977954
View Table of Contents: http://aip.scitation.org/toc/jap/121/10
Published by the American Institute of Physics

Photoluminescence enhancement of ZnO via coupling with surface plasmons on Al thin films

S. Dellis,[1,2] N. Kalfagiannis,[2] S. Kassavetis,[1] C. Bazioti,[1] G. P. Dimitrakopulos,[1] D. C. Koutsogeorgis,[2,a)] and P. Patsalas[1,a)]
[1]*Department of Physics, Aristotle University of Thessaloniki, Thessaloniki GR-54124, Greece*
[2]*School of Science and Technology, Nottingham Trent University, Nottingham NG11 8NS, United Kingdom*

(Received 20 October 2016; accepted 20 February 2017; published online 10 March 2017)

We present that the ultra-violet emission of ZnO can be enhanced, as much as six-times its integral intensity, using an Al thin interlayer film between the Si substrate and ZnO thin film and a post-fabrication laser annealing process. The laser annealing is a cold process that preserves the chemical state and integrity of the underlying aluminum layer, while it is essential for the improvement of the ZnO performance as a light emitter and leads to enhanced emission in the visible and in the ultraviolet spectral ranges. In all cases, the metal interlayer enhances the intensity of the emitted light, either through coupling of the surface plasmon that is excited at the Al/ZnO interface, in the case of light-emitting ZnO in the ultraviolet region, or by the increased back reflection from the Al layer, in the case of the visible emission. In order to evaluate the process and develop a solid understanding of the relevant physical phenomena, we investigated the effects of various metals as interlayers (Al, Ag, and Au), the metal interlayer thickness, and the incorporation of a dielectric spacer layer between Al and ZnO. Based on these experiments, Al emerged as the undisputable best choice of metal interlayers because of its compatibility with the laser annealing process, as well as due to its high optical reflectivity at 380 and 248 nm, which leads to the effective coupling with surface plasmons at the Al/ZnO interfaces at 380 nm and the secondary annealing of ZnO by the back-reflected 248 nm laser beam. *Published by AIP Publishing.* [http://dx.doi.org/10.1063/1.4977954]

I. INTRODUCTION

The advancements in growing and controlling the electrical and optical properties of ZnO, the archetypical oxide semiconductor, have created new opportunities and have revolutionized the Thin Film Transistor (TFT),[1] Light Emitting Diode (LED),[2] and Solid State Diode Laser (SSDL)[3] technologies. This has been boosted mainly by the extraordinary combination of ZnO's assets, such as its chemical stability (enthalpy of formation $\Delta_f H^o = -348$ kJ/mol), abundance of constituent elements, a direct optical band gap ($E_g = 3.34$ eV), comparable to that of GaN,[4] its inherent *n*-type character,[5] and the ability to fabricate it using a variety of methods such as magnetron sputtering,[6] molecular beam epitaxy,[7] metalorganic chemical vapor deposition,[8] and spray pyrolysis.[9]

A major asset of ZnO is that its Photoluminescence (PL) spectra consist of two emission components: a narrow Ultra-Violet (UV) peak at around 380 nm, which is correlated with the near band-edge (NBE) exciton emission,[10] and a broad visible (VIS) peak spanning from 450 to 750 nm, which is associated with deep level emission (DLE) from intrinsic and extrinsic defects.[11–14] The fabrication of high-quality ZnO films with strong UV or VIS emission is a challenging task; a high-temperature deposition or/and a post-deposition annealing scheme is usually required[15,16] with thermal annealing[17] and rapid thermal annealing,[18] which however are not compatible with temperature sensitive underlayers, such as thin metal layers. Consequently, laser annealing[19,20] (LA), being a cold process, is a favourable alternative for processing such structures. Specifically, Tsakonas *et al*. have presented the superiority of laser annealing, for the fabrication of high-intensity UV emitting ZnO, due to the nature of laser annealing, being an ultra-fast approach, allowing precise delivery of energy to the constituents and being compatible with large area processing.[20] They have concluded that LA can control the microstructure, defect density, luminescence properties, surface morphology, and internal strain/film stress in ZnO. The resultant DLE/NBE emissions are directly correlated with LA processing parameters, consistent with the optical absorption properties of the films, as well as with the structural changes occurring after LA (e.g., the as-deposited ZnO films do not exhibit any PL whatsoever; they are polycrystalline with fine grains, 10–15 nm, and high in-grain defect density; after LA with a fluence of 238 mJ/cm^2, their grain size was enlarged to 10–40 nm but still with high in-grain defect density and exhibit significant DLE; after LA with a fluence of 295 mJ/cm^2, their microstructure is transformed to columnar with 60 nm long columns, with a diameter of 15–25 nm, very thin grain boundaries, and a very low defect density, exhibiting very strong NBE).[20] However, the NBE emission intensity that can be achieved by LA is still below the desired level for UV light emitting devices; thus, the emission efficiency of ZnO has to be substantially increased.[21] Recently, surface plasmon (SP) excitations at semiconductor/metal (usually metal is Ag) interfaces have been exploited for the enhancement of PL in emitting devices.[22–24] This is based on the introduction

a)Authors to whom correspondence should be addressed. Electronic addresses: ppats@physics.auth.gr, Tel.: +30-2310-998298 and Demosthenes.koutsogeorgis@ntu.ac.uk, Tel.: +44-115-8488334.

of a thin nanostructured metal layer in a light emitting device that results in the loss of much of the momentum of SP modes, thus increasing their ability to couple with light.[25] Okamoto *et al.*[22] first claimed that the same effect can originate from the inherent surface roughness of the evaporated Ag film. Furthermore, You *et al.*[26] have presented the enhancement of the PL intensity of ZnO when grown on top of an Ag thin film and studied the influence of the morphology of the deposited Ag film. In this study, it was shown that a higher surface roughness density, defined as the root mean square (RMS) roughness per grain area, can lead to larger emission enhancement. Finally, the influence of an Al thin film (with and without the presence of an AlO_x capping layer) on the PL of ZnO thin films has been studied by several research groups.[27–29] These studies show that an Al thin film in the vicinity of a luminescent material, like ZnO, can lead to an increase in its UV emission through the coupling between excitons and SPs of Al.

In the present work, we investigate the UV-VIS emission of ZnO thin films fabricated on top of a metal layer and post-processed by LA. LA is used to modify the structural quality of the ZnO at low macroscopic temperatures[30] and consequently the balance of NBE and DLE emission as well while retaining the chemical state and the integrity of the underlying plasmonic metal layer. The most common plasmonic metals, Au, Ag, and Al, were tested as interlayer films between the sputtered ZnO and the Si substrate. By comparison, we lead to the selection of Al as a plasmonic interlayer of choice, despite its chemical sensitivity and low melting point, as its use resulted in high-intensity emitted light, both in the UV and VIS regions after LA for different physical reasons.

II. EXPERIMENTAL

The sample preparation comprised three steps. First, *n*-type Si (100) wafers were coated by metal thin films of different thicknesses employing the RF magnetron sputtering technique. Three different types of substrates (Al-covered, Au-covered, and Ag-covered Si) were prepared. The films' deposition was performed in an Ar atmosphere with the pressure settled at 5 mTorr and the power at 0.27 W/cm^2 at room temperature. The use of Ag, Au, and Al thin films stems from the fact that all three of them exhibit well-known plasmonic behaviors. Then, a 60 nm thick ZnO film was deposited on top of the metal thin film using a ZnO target (3″ in diameter). The deposition was done in a second sputtering chamber and in a mixed O_2/Ar environment (20% O_2 in Ar, partial pressure of the mixture: 2 mTorr) with the RF power set at 0.27 W/cm^2 at room temperature. The influence of a passive spacer layer between the metal and ZnO thin film was studied by the introduction of an additional deposition step in the sample's fabrication process. Specifically, the metal thin film was covered by a polycrystalline w-AlN (i.e., hexagonal wurtzite-type AlN) thin film that was deposited *in-situ* (i.e., without exposure of the metal surface to the lab atmosphere, thus, ensuring that the w-AlN/Al interface would be optimal and ultra-clean.) by RF magnetron sputtering, as well. The deposition of w-AlN was done in a mixed N_2/Ar environment (25% N_2 in Ar, partial pressure of the mixture was 7.5 mTorr) with the use of an Al target and the RF power set at 1.5 W/cm^2 at room temperature. Finally, the whole structure was subjected to LA with a single laser pulse. LA of the samples was carried out by employing a KrF excimer laser (LAMDA PHYSIK-LPX 305i) delivering pulses of 248 nm with 25 ns duration.[30] The beam delivery system consists of a variable attenuator, a beam homogenizer, and a mask projection system, resulting in a homogenized square laser beam of 2.5 × 2.5 mm^2. Before the laser beam hits the sample, it was splitted into two parts with the use of a laser beam splitter guiding a part of the beam to an energy monitor. This setup allows the measurement of the fluence of each pulse separately. For this reason, every emission spectrum is attributed to a single laser annealed area. In order to test the consistency of the laser annealing influence on the PL emission of ZnO, several areas of the same samples were irradiated with a single pulse of the fluence resulting in the highest NBE, indicating that the NBE intensity was approximately the same for small fluence variations (in the range of 1 mJ/cm^2). PL and Transmission Electron Microscopy (TEM) were used for the study of the luminescence of all samples and of the morphology/structure of the LA Al/ZnO bi-layers, respectively. For the PL measurements, both the excitation and the emitted light collection took place from the ZnO side (the detection probe was placed normal to the surface) using a He-Cd continuous wave laser (325 nm) of 9 mW as an excitation source.

The morphological features of the Al surfaces were obtained by Atomic Force Microscopy (AFM). The AFM measurements were performed with a Dimension Icon Scanning Probe Microscope (Bruker). AFM was mounted in an anti-vibration air stable granite stage installed inside an acoustic enclosure. The standard tapping mode was utilized for better image acquisition using extra sharp pyramidal silicon cantilevers to reduce the AFM's minimum detectable size (nominal tip radius: 8 nm) with a force constant of 42 N/m. 1 × 1 μm^2 images were obtained, and the RMS roughness was estimated/calculated through appropriate imaging analysis.

Transmission electron microscopy (TEM) observations were performed using a 200 kV JEOL JEM 2000FX microscope. Sample preparation was performed by tripod polishing followed by Ar^+ ion milling.

III. RESULTS AND DISCUSSION

It has previously been presented that the LA of a ZnO thin film has a great influence on its PL emission.[20] The key parameter of this process is the fluence of the applied laser pulse. Specifically, the as-grown sputtered Si/ZnO films of this study do not exhibit initially any PL at all due to their very low crystalline quality. A narrow laser processing fluence window is adequate to promote PL either in the UV (higher fluence) or in the VIS (lower fluence) spectral range. This is vividly illustrated in Fig. 1. Indeed, low laser fluences (up to 215 mJ/cm^2) do not promote any PL at all. At approximately 250 mJ/cm^2, DLE emerges, while for fluences above 260 mJ/cm^2, the NBE emission emerges in the expense of DLE. This is probably due to grain sintering in ZnO and the elimination of defects, respectively. For fluences beyond approximately 300 mJ/cm^2 (where the maximum NBE is

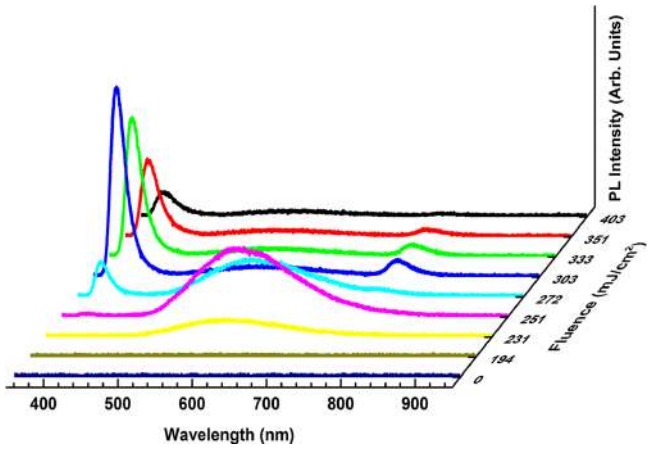

FIG. 1. PL spectra of LA-processed ZnO thin films with a single pulse of the 248 nm beam at various fluence values.

observed), the NBE emission deteriorates due to overheating and damage (possibly also due to ablation) of ZnO.

Further enhancement of the UV emission intensity can be achieved by the introduction of a metal thin film between the ZnO and the Si substrate. This enhancement of the PL emission of ZnO is expected to be the result of a two-step mechanism. The energy excited in the ZnO is not transferred to photons but into SPs excited in the Al/ZnO interface, and then SPs emit light if the momentum matching condition is fulfilled.[22,24,26] This enhancement is expected to become higher through the increase of the density of the SP states; the selection of the appropriate metal is needed in order to achieve high NBE enhancement. For this reason, the surface plasmon polariton (SPP) dispersion at the metal/ZnO interface for Ag, Al, and Au was calculated by considering the following dispersion equation:[31]

$$\hbar k_x = \frac{\hbar\omega}{c}\sqrt{\frac{\varepsilon_m \varepsilon_d}{\varepsilon_m + \varepsilon_d}}, \tag{1}$$

where k_x is the wave vector of the surface plasmon, ε_m and ε_d are the dielectric constants of the metal and dielectric medium, respectively, and $\hbar\omega$ is the incident photon energy. The dielectric constants for all the considered metals and ZnO were derived from Spectroscopic Ellipsometry (SE) measurements of single-layer thick films of Au, Ag, Al, and ZnO deposited by sputtering and therefore include realistic electron losses. As Fig. 2 shows, the plasmon energy (being the photon energy that corresponds to the maximum finite wave-vector)[31] of Ag and Au covered by ZnO is approximately 2.9 eV and 2.1 eV, i.e., blue and red lines, respectively. It is evident that Ag can hardly sustain an SPP from photons originating from the NBE emission of ZnO (also shown in Fig. 2 as a magenta line), while Au cannot sustain such an SPP at all. On the contrary, the Al dispersion curve (Fig. 2, green line) crosses the energy of the emitted NBE photons and can get longer wave-numbers for higher photon energies, thus being able to probe SPPs at the Al/ZnO interface.

As we mentioned previously, the low SPP's energy of Au compared to the ZnO band-gap makes it unsuitable for use in the enhancement of ZnO UV (NBE) emission. Indeed, this was confirmed by the absence of any enhancement of

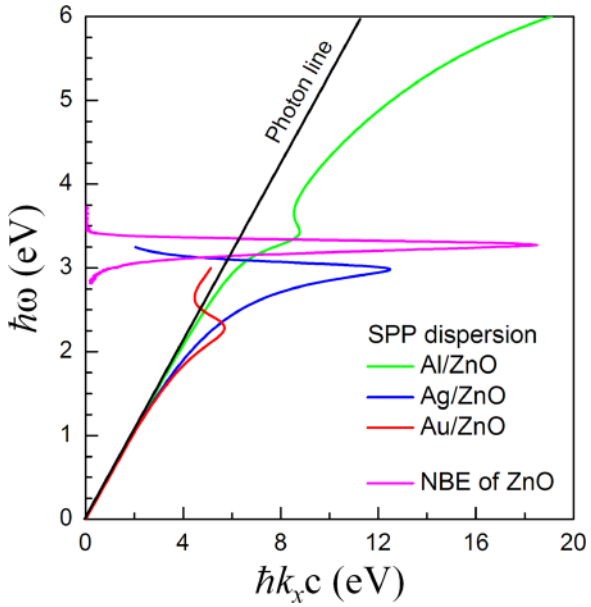

FIG. 2. Dispersion curves of the SPP at the metal/ZnO interface. The NBE emission of laser annealed ZnO is also presented in the diagram (magenta solid line).

NBE emission in the PL emission of LA ZnO deposited on top of an approximately 80 nm thick Au film (not shown). In addition, the SPP energy of Ag is close to the ZnO band gap, but Ag is incompatible with the LA process. In particular, when an 80 nm thick Ag film was used as an interlayer, the ZnO is ablated for fluence as low as 100 mJ/cm^2, meaning that the ablation due to Ag occurs before the structural modifications of the ZnO, which are responsible for the emergence of NBE of the ZnO layer itself. The penetration depth of the 248 nm laser beam on ZnO has been experimentally calculated to be approximately 120 nm,[20] leading to the 60 nm ZnO thin film being semitransparent to the 248 nm beam and part of the beam's energy to be delivered to the underlying metal; Al is reflective at 248 nm, while Ag is absorbing resulting in different laser-matter interactions at 248 nm, which explains the difference in compatibility of the two interlayer metals with the LA process. The high absorbance of 248 nm light from Ag results in the increase in the Ag temperature and dewetting with subsequent ablation of the ZnO. This is in contrast to the Al interlayer, whose SPP dispersion also crosses the NBE emission of ZnO (Fig. 2) and appears as the only viable candidate interlayer for the plasmonic enhancement of UV PL from ZnO-based devices.

For the study of the influence of the underlying Al thin films on the PL emission of ZnO, we enlisted various thicknesses of Al thin films, namely, 15, 20, 50, and 75 nm. These Si/Al structures were used as substrates for the deposition of a 60 nm thick ZnO film that was subsequently laser annealed with the appropriate conditions in order to achieve optimized DLE or NBE emission. It has to be noted that the ZnO film on top of Al presents the same behavior under LA with the ZnO films fabricated on top of Si;[15] albeit lower fluences are necessary in this case to achieve the highest DLE and NBE emission. This is probably due to the back-reflection of the 248 nm processing laser light by the Al layer (Al exhibits

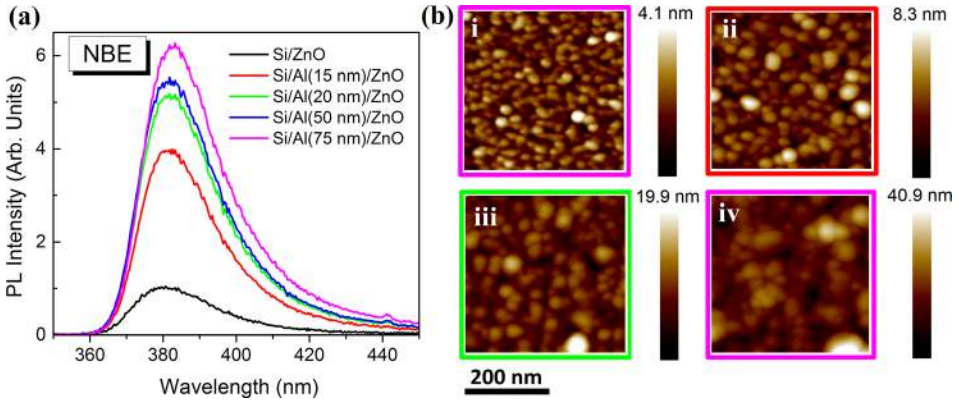

FIG. 3. (a) PL emission spectra of the LA-processed ZnO and Al/ZnO bilayer samples that present the highest NBE (LA at 270 mJ/cm^2); (b) AFM images of the (i) 15, (ii) 20, (iii) 50, and (iv) 75 nm thick Al films' surface before the deposition of ZnO (for larger images, see Figure S1 of the supplementary material).

92% reflectivity at 248 nm), leading to a second successive round of LA through the thin ZnO film (accounting also for the fact that the penetration depth of the 248 nm beam into ZnO is 130 nm (Ref. 20)).

Figure 3(a) presents the PL spectra of the LA Si/Al/ZnO trilayers where the highest NBE peak for the various Al thin film thicknesses, achieved after a single pulse at 270 mJ/cm^2 in all cases, are manifested. The existence of an Al thin interlayer between ZnO and Si leads to the enhancement of the NBE intensity. The inset of Fig. 4 shows (solid purple curve) that the enhancement factor increases as the thickness of the Al thin film increases, reaching its highest value of 6.3, when an Al interlayer of 75 nm thickness (the thickest Al film used in this study) is introduced between the Si substrate and the ZnO thin film. The enhancement of the NBE intensity can be attributed to the strong interaction with SPs. SPs can be excited by the emitted light from the ZnO thin film and propagate along the Al/ZnO interface. By scattering at the surface roughness of the film, the SPs decay and the carried energy is reformed again to light emission.[32–36] Through this radiative decay channel, the intensity of the NBE emission of the ZnO film is substantially increased. Given that the skin depth into the Al layer is far less than 50 nm, the PL enhancement for the cases of 50 and 70 nm thick Al layers strongly indicates that the increase in the enhancement factor with the film thickness might be the result of the increased surface roughness, thus leading to higher enhancement of the NBE emission of ZnO due to the larger number of scattering centers.[27] This assumption is supported by the study of the morphological features of the Al thin film before the deposition of ZnO by AFM shown in Fig. 3(b). The RMS value for each Al film thickness was calculated by the AFM images, and it increases from 0.581 nm for the 15 nm thick Al film to 5.220 nm for the 75 nm thick Al thin film (larger AFM images of the Al thin films and the results of their quantitative analysis are presented in Figs. S1 and S2 in supplementary material).

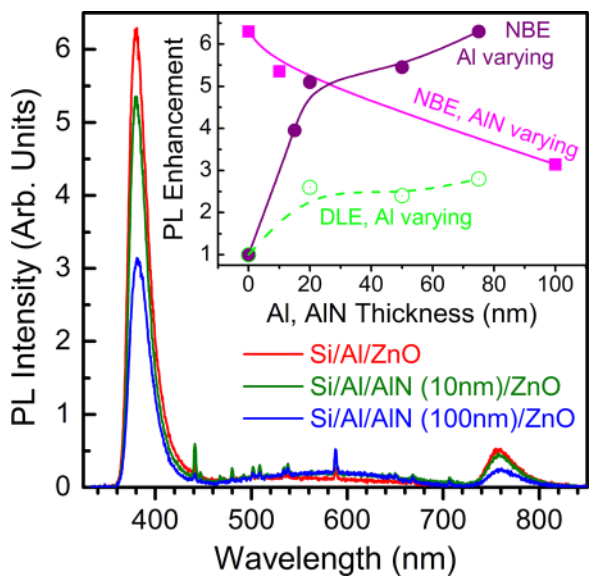

FIG. 4. PL spectra from LA-processed Si/Al/ZnO, Si/Al/AlN(10 nm)/ZnO, and Si/Al/AlN(100 nm)/ZnO structures (in all cases, the thickness of Al is 75 nm); inset: enhancement factor of NBE and DLE *vs.* the thickness of Al (purple and green lines respectively) or AlN (magenta line) for Si/Al/ZnO and Si/Al(75 nm)/AlN/ZnO structures, respectively.

In order to prove that the observed enhancement of the NBE PL originates from the SPs at the ZnO/Al interface, we considered the implementation of a dielectric spacer layer between ZnO and Al. As a dielectric spacer, we used w-AlN, which has a band gap of 6.2 eV s. w-AlN thin films of 10 and 100 nm thickness were deposited *in situ* on top of a 75 nm thick Al film, resulting in the preparation of a third type of samples (Si/Al/AlN/ZnO), in addition to the other two types (Si/ZnO and Si/Al/ZnO) that were studied in the previous paragraphs. All three types of samples were subsequently laser annealed with the appropriate conditions in order to achieve the highest NBE emission (the highest NBE emission in samples with an AlN/Al bilayer below the ZnO thin film was achieved with approximately the same fluence as with the case of the pure Al interlayer). Figure 4 compares the PL spectra for the cases of Si/Al/ZnO, Si/Al/AlN(10 nm)/ZnO, and Si/Al/AlN(100 nm)/ZnO for a 75 nm thick Al layer. It is evident that the maximum NBE enhancement occurs for the Si/Al/ZnO structure, and then it is substantially reduced with increasing AlN spacer interlayer thickness (inset of Fig. 4, magenta curve). Considering that the SP field penetration depth (Z) into the AlN is given by[31]

$$Z = \frac{\lambda}{2\pi}\left|\frac{\varepsilon_{AlN} + \varepsilon'_{Al}}{\varepsilon^2_{AlN}}\right|^{1/2}, \tag{2}$$

where ε'_{AlN} is the dielectric constant of AlN and ε'_{Al} are the real parts of the dielectric constants of Al, the penetration depth into AlN is calculated to be equal to 48 nm. Thus, the

reduction in the enhancement factor with the increasing thickness of AlN is the direct consequence of the weakening of the SP field within it. This is a firm proof of the hypothesis that the enhancement of the ZnO NBE emission comes from its coupling with the SPs, excited at the Al/ZnO interface. Finally, the moderate enhancement of NBE for the 100 nm AlN spacer (i.e., thicker than the SP's field penetration depth) is attributed exclusively to the back-reflection of the emitted photons from the ZnO layer by the Al mirror layer. The relative strengths of the NBE peaks for Si/Al/ZnO (red line) and Si/Al/AlN(100 nm)/ZnO (blue line) may be used to quantify the contributions of these two mechanisms (SP and back-reflection) to the NBE PL enhancement.

The Al interlayers present also high reflectivity values in the spectral range where the visible DLE emission occurs. In Fig. 5, we observe that the incorporation of the Al layer between Si and ZnO results in the increase of DLE PL after LA (with a fluence of 220 mJ/cm^2). An enhancement factor close to 3, in relation to the reference sample (Si/ZnO), is observed in the inset of Fig. 4. The enhancement factor of DLE is independent of the Al thin film thickness (Fig. 5), suggesting that it most likely originates from the back reflection of the PL excitation beam and the emitted photons rather than from probing SPs at the Al/ZnO interface. This is further supported by the fact that the enhancement factor for DLE from Si/Al/ZnO is comparable to the enhancement factor of NBE for Si/Al/AlN/ZnO where no SP coupling occurs (i.e., for a 100 nm thick AlN, see inset of Fig. 4), given that the reflectivity of Al is almost constant in the visible and UV spectral ranges.

In order to visualize the morphological and structural changes that occur in Si/Al/ZnO heterostructures after LA and result in the substantial enhancement of either the NBE or DLE PL bands, we performed cross-sectional TEM experiments in as-grown (Fig. 6(a)) and laser annealed Si/Al/ZnO samples with fluences of 250 and 300 mJ/cm^2 that promote the DLE and NBE, respectively (Figs. 6(b) and 6(c), respectively). For the as-grown sample, both Al and ZnO layers are nanocrystalline, exhibiting columnar crystallites as illustrated in Fig. 6(a). The ZnO film exhibits nanoscale roughness both at the film surface, as well as at the interface with the Al layer. Part of the Al/ZnO interfacial region appears amorphous and may have been amorphized through oxidation of the aluminum. After LA, the Al layer is continuous and does not show any columnar structure, as it is shown in Figs. 4(b) and 4(c) for the LA fluences of 250 and 300 mJ/cm^2 that promote the DLE and NBE, respectively. This is most likely due to Al melting upon LA and re-solidification. The sample with the highest NBE peak (Fig. 6(c)) has a smoother surface, providing the conditions for the creation of an SP, but exhibits larger surface undulations. In contrast, the surface of the sample that presented the highest DLE peak (Fig. 6(b)) exhibits larger features compared to the other two. From dark field TEM images of untreated and laser treated Al/ZnO bilayers (not presented), it was found that the grain boundaries in the Al layer diminished following LA due to the imposed re-crystallization. A small increase in ZnO nanocolumn size after annealing that may be attributed to grain re-orientations and elimination of extended defects is also observed, especially for the NBE case (Fig. 6(c)). The quality of ZnO crystallites improved after LA, as the ZnO rings observed on selected area electron diffraction patterns appeared sharper, explaining the NBE existence for the case of the Si/ZnO, as well. Therefore, we might safely propose that the LA process is beneficial for both the homogeneity of the Al interlayer and the structural features of ZnO, which are the source of NBE and DLE, while its effect on the interfacial (Al/ZnO) roughness is minor. Last but not least, the TEM observation clearly demonstrated that the Al interlayer can endure the LA process, making Al not only optically appropriate but also an LA-compatible and viable interlayer for plasmon-enhanced, ZnO-based devices.

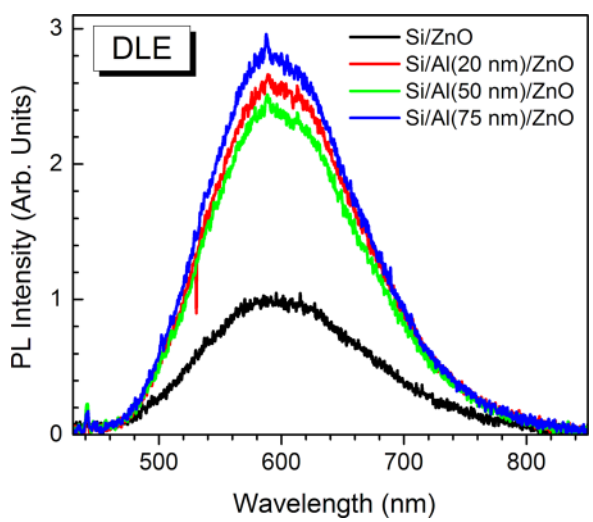

FIG. 5. PL emission of the LA-processed ZnO and Al/ZnO samples that present the highest DLE (LA at 220 mJ/cm^2).

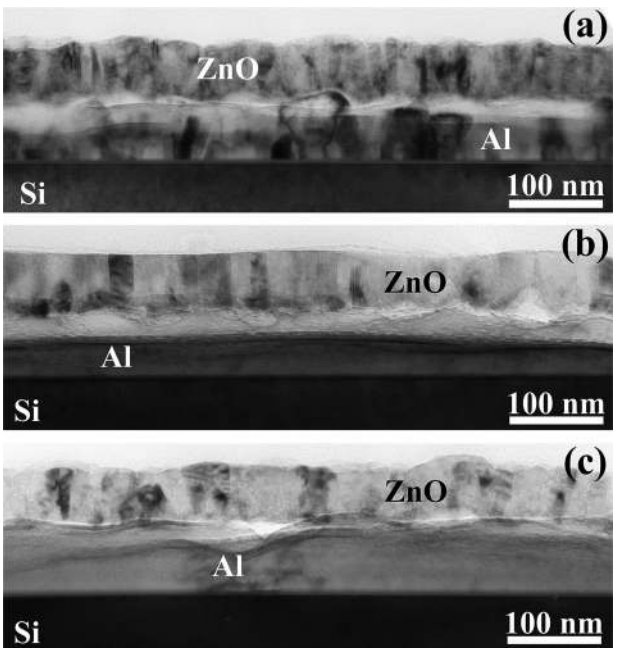

FIG. 6. Bright field (BF) TEM images of the (a) untreated, (b) high DLE, and (c) high NBE LA-processed ZnO/Al/Si observed along the [110] Si zone axis.

IV. CONCLUSIONS

In conclusion, the enhancement of the UV emission of ZnO thin films by the introduction of an Al thin film between the ZnO and the substrate, as well as employing a post-fabrication laser annealing process, has been studied and evaluated. It was shown that there is an LA processing window where the applied laser beam fluence can tailor the PL components of metal/ZnO bilayers, namely, the NBE and DLE peaks. The NBE component of the Al/ZnO bi-layer is enhanced by a factor exceeding six in comparison to the NBE emission of a purely ZnO thin film and shows a strong dependence on the Al thickness, due to the SPs at the Al/ZnO interface; the quality of the interface has been evaluated by atomic force microscopy via measuring the Al roughness before the ZnO deposition and was found to affect the PL enhancement. In addition, a strong and enhanced (by approximately a factor of three) DLE component appears when the Al/ZnO bilayer is laser-annealed with an appropriate laser fluence. The enhancement of the DLE emission is unrelated to the Al thin film thickness and is the consequence of the back-reflection of the emitted photons. The use of Ag and Au thin films as interlayer films was also studied in order to find the optimum material combination. From this investigation, it was derived that, in terms of the UV emission intensity enhancement, as well as the durability during the laser annealing process, Al is the undisputable material of choice.

SUPPLEMENTARY MATERIAL

See supplementary material for the surface morphology of the Al layers studied by AFM and for a table with the details of the sputter growth of the films.

ACKNOWLEDGMENTS

The authors gratefully acknowledge fruitful discussions and review comments by Professor E. Lidorikis of the University of Ioannina. S. Dellis acknowledges funding from the Erasmus$^+$ Programme. N. Kalfagiannis acknowledges funding from the People Programme (Marie Curie Actions) LASER-PLASMON of the European Union's Seventh Framework Programme (FP7/2007-2013) under REA Grant Agreement No. PIEF-GA-2012-330444.

[1]P. F. Carcia, R. S. McLean, M. H. Reilly, and G. Nunes, Appl. Phys. Lett. **82**, 1117 (2003).
[2]O. Lupan, T. Pauporté, and B. Viana, J. Phys. Chem. C **114**, 14781 (2010).
[3]M. Kawasaki, Mater. Sci. Eng. B **56**, 239 (1998).
[4]Ü. Özgür, Y. I. Alivov, C. Liu, A. Teke, M. A. Reshchikov, S. Doğan, V. Avrutin, S. J. Cho, and H. Morkoç, J. Appl. Phys. **98**, 1 (2005).
[5]S. B. Zhang, S.-H. Wei, and A. Zunger, Phys. Rev. B **63**, 1 (2001).
[6]E. Kayahan, J. Lumin. **130**, 1295 (2010).
[7]Z. K. Tang, G. K. L. Wong, P. Yu, M. Kawasaki, A. Ohtomo, H. Koinuma, and Y. Segawa, Appl. Phys. Lett. **72**, 3270 (1998).
[8]Y. Liu, C. R. Gorla, S. Liang, N. Emanetoglu, Y. Lu, H. Shen, and M. Wraback, J. Electron. Mater. **29**, 69 (2000).
[9]G. Adamopoulos, S. Thomas, D. D. C. Bradley, M. A. McLachlan, and T. D. Anthopoulos, Appl. Phys. Lett. **98**, 123503 (2011).
[10]W. Shan, W. Walukiewicz, J. W. Ager III, K. M. Yu, H. B. Yuan, H. P. Xin, G. Cantwell, and J. J. Song, Appl. Phys. Lett. **86**, 191911 (2005).
[11]H. Gao, J. Teng, and S. J. Chua, J. Appl. Phys. **119**, 13104 (2016).
[12]A. B. Djurišić, Y. H. Leung, K. H. Tam, L. Ding, W. K. Ge, H. Y. Chen, and S. Gwo, Appl. Phys. Lett. **88**, 103107 (2006).
[13]T. Matsumoto, H. Kato, K. Miyamoto, M. Sano, E. A. Zhukov, and T. Yao, Appl. Phys. Lett. **81**, 1231 (2002).
[14]B. Lin, Z. Fu, and Y. Jia, Appl. Phys. Lett. **79**, 943 (2001).
[15]J. H. Lim, C. K. Kong, K. K. Kim, I. K. Park, D. K. Hwang, and S. J. Park, Adv. Mater. **18**, 2720 (2006).
[16]D. Thapa, J. Huso, J. L. Morrison, C. D. Corolewski, M. D. McCluskey, and L. Bergman, Opt. Mater. **58**, 382 (2016).
[17]H. S. Kang, J. S. Kang, S. S. Pang, E. S. Shim, and S. Y. Lee, Mater. Sci. Eng., B: Solid-State Mater. Adv. Technol. **102**, 313 (2003).
[18]S. P. Ghosh, K. C. Das, N. Tripathy, G. Bose, D. H. Kim, T. I. Lee, J. M. Myoung, and J. P. Kar, J. Mater. Sci.: Mater. Electron. **26**, 7860 (2015).
[19]K. Kim, S. Kim, and S. Y. Lee, Curr. Appl. Phys. **12**, 585 (2012).
[20]C. Tsakonas, W. Cranton, F. Li, K. Abusabee, A. Flewitt, D. Koutsogeorgis, and R. Ranson, J. Phys. D: Appl. Phys. **46**, 95305 (2013).
[21]D.-K. Hwang, M.-S. Oh, J.-H. Lim, and S.-J. Park, J. Phys. D: Appl. Phys. **40**, R387 (2007).
[22]K. Okamoto, I. Niki, A. Shvartser, Y. Narukawa, T. Mukai, and A. Scherer, Nat. Mater. **3**, 601 (2004).
[23]J. B. You, X. W. Zhang, Y. M. Fan, S. Qu, and N. F. Chen, Appl. Phys. Lett. **91**, 231907 (2007).
[24]W. L. Barnes, Nat. Mater. **3**, 588 (2004).
[25]P. A. Hobson, S. Wedge, J. A. E. Wasey, I. Sage, and W. L. Barnes, Adv. Mater. **14**, 1393 (2002).
[26]J. B. You, X. W. Zhang, Y. M. Fan, Z. G. Yin, P. F. Cai, and N. F. Chen, J. Phys. D: Appl. Phys. **41**, 205101 (2008).
[27]D. Y. Lei, L. Zhang, and H. C. Ong, ACS Appl. Mater. Interfaces **7**, 23496 (2015).
[28]Y. Fang, Y. Wang, L. Gu, R. Lu, and J. Sha, Opt. Express **21**, 3492 (2013).
[29]J. Li and H. C. Ong, Appl. Phys. Lett. **92**, 121107 (2008).
[30]N. Kalfagiannis, A. Siozios, D. V. Bellas, D. Toliopoulos, L. Bowen, N. Pliatsikas, W. M. Cranton, C. Kosmidis, D. C. Koutsogeorgis, E. Lidorikis, and P. Patsalas, Nanoscale **8**, 8236 (2016).
[31]S. A. Maier, *Plasmonics: Fundamentals and Applications* (Springer US, Boston, MA, 2007).
[32]E. Kretschmann and H. Raether, Zeitschrift für Naturforschung A **23**, 2135 (1968).
[33]E. Ferlenghi and M. Iannuzzi, Phys. Lett. A **32**, 238 (1970).
[34]E. Kretschmann, Opt. Commun. **6**, 185 (1972).
[35]I. Lindau and P. O. Nilsson, Phys. Lett. A **31**, 352 (1970).
[36]R. Orlowski and H. Raether, Surf. Sci. **54**, 303 (1976).

Photoluminescence Enhancement of ZnO via Coupling with Surface Plasmons on Al Thin Films

S. Dellis[1,2], N. Kalfagiannis[2], S. Kassavetis[1], C. Bazioti[1], G.P. Dimitrakopulos[1], D.C. Koutsogeorgis[2,a], and P. Patsalas[1,1]

[1]Department of Physics, Aristotle University of Thessaloniki, Thessaloniki, GR-54124, Greece

[2]School of Science and Technology, Nottingham Trent University, Nottingham, NG11 8NS, United Kingdom

Supporting Information

I. Surface Morphology of the Al layers

Figure S1 shows the AFM images from four sputtered Al of varying thickness. It is clearly shown that the root mean square roughness (RMS) of the Al surfaces is increasing with increasing of the Al thin film thickness. From AFM images analysis the RMS of 15nm, 20 nm, 50 nm, and 75 nm thick Al films was estimated equal to 0.581 nm, 1.150 nm, 2.530, and 5.220 nm, respectively. The roughness-thickness correlation is presented in Fig. S2.

[1]Authors to whom correspondence should be addressed:
P. Patsalas, Electronic mail: ppats@physics.auth.gr, tel: +30-2310-998298.
D.C. Koutsogeorgis, Electronic mail: Demosthenes.koutsogeorgis@ntu.ac.uk, tel: +44-115-8488334.

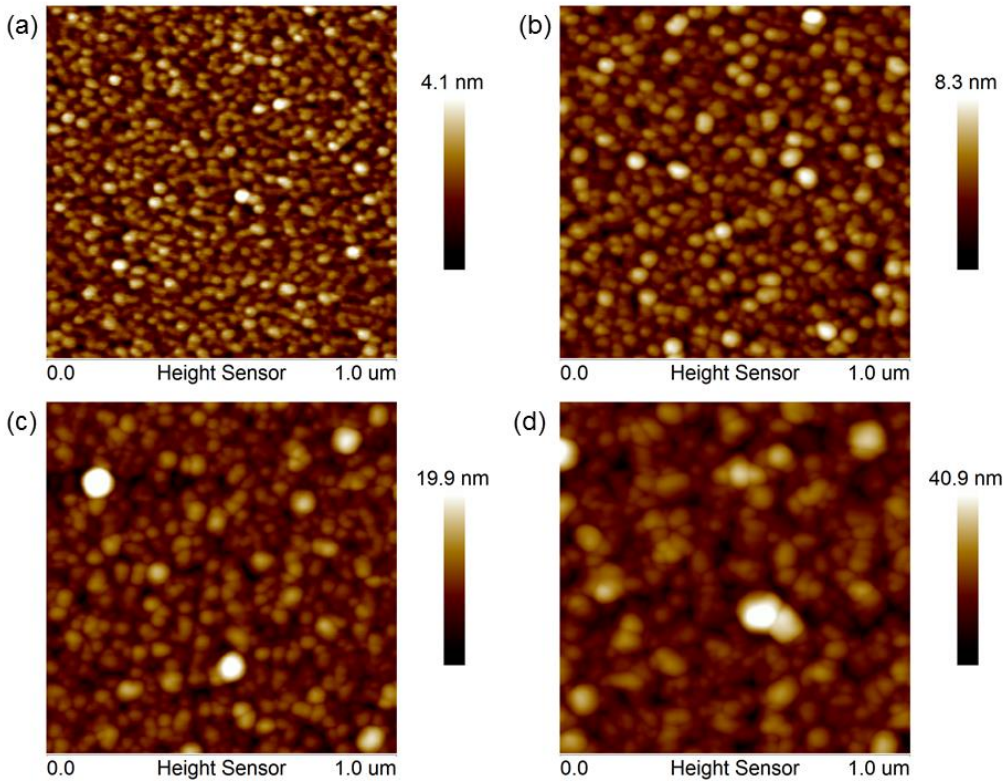

FIG. S1: AFM images of (a) 15 nm, (b) 20 nm, (c) 50 nm, and (d) 75 nm thick Al thin film before the deposition of ZnO thin film.

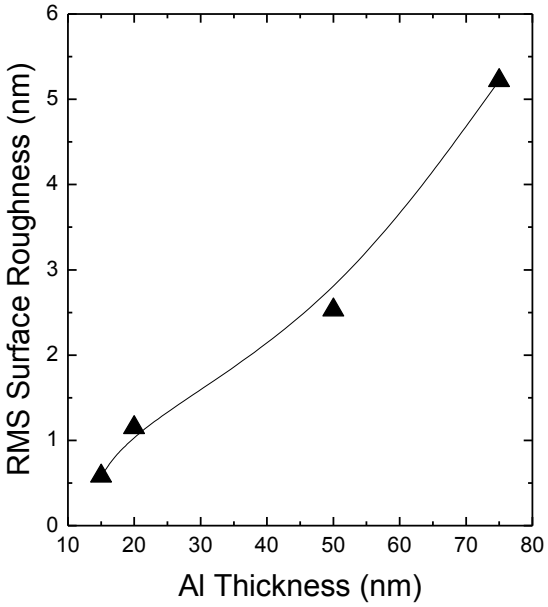

FIG. S2: The evolution of the root mean square (RMS) roughness *vs.* the Al film thickness as determined by AFM.

II. Details of the sputter growth of thin films

The deposition parameters of every type of thin films used for the preparation of the samples of this study are presented in Table S1.

Table S1. Parameters of the deposition of each material used for the samples preparation.

Deposited Material	**Base Pressure (mbar)**	**Working Pressure (mTorr)**	**Deposition Environment**	**Power Density (W/cm^2)**
ZnO	$\approx 10^{-7}$	2	20% O_2 in Ar	0.27
AlN	$3 \cdot 10^{-6}$	7.5	25% N_2 in Ar	1.5
Al	$3 \cdot 10^{-6}$	5	Ar	0.27
Au	$3 \cdot 10^{-6}$	5	Ar	0.27
Ag	$3 \cdot 10^{-6}$	5	Ar	0.27